Description and Characterization of the *Odontella aurita* OAOSH22, a Marine Diatom Rich in Eicosapentaenoic Acid and Fucoxanthin, Isolated from Osan Harbor, Korea

Sung Min An , Kichul Cho , Eun Song Kim , Hyunji Ki , Grace Choi , Nam Seon Kang *

Posted Date: 30 September 2023

doi: 10.20944/preprints202309.1848.v1

Keywords: Carotenoid pigments; Fatty acids; Odontella aurita; Optimal growth condition; Ultrastructure; 18S rDNA

Article

Description and Characterization of the *Odontella aurita* OAOSH22, a Marine Diatom Rich in Eicosapentaenoic Acid and Fucoxanthin, Isolated from Osan Harbor, Korea

Sung Min An, Kichul Cho, Eun Song Kim, Hyunji Ki, Grace Choi and Nam Seon Kang*

Department of Microbial Resources, National Marine Biodiversity Institute of Korea, Seocheon 33662, Republic of Korea
* Correspondence: kang3610@mabik.re.kr

Abstract: Third-generation biomass production utilizing microalgae exhibits sustainable and environmentally friendly attributes, along with significant potential as a source of physiologically active compounds. However, the process of screening and localizing strains that are capable of producing high-value-added substances necessitates a significant amount of effort. In the present study, we have successfully isolated the indigenous marine diatom *Odontella aurita* OAOSH22 from the East coast of Korea. Subsequently, we conducted a comprehensive analysis of its morphological, molecular, and biochemical characteristics. Afterwards, comprehensive analysis was conducted on the morphological, molecular, and biochemical characteristics, along with testing for optimal growth conditions. The morphological characteristics of the isolate were observed using optical and electron microscopes, and it exhibited typical features of *O. aurita*. Additionally, the molecular phylogenetic inference derived from the sequence of the small-subunit 18S rDNA confirmed the classification of the microalgal strain as *O. aurita*. This isolate has been confirmed to contain 7.1 mg g^{-1} dry cell weight (DCW) of fucoxanthin, a powerful antioxidant substance, in terms of dry cell weight (DCW). In addition, this isolate contains 11.1 mg g^{-1} DCW of eicosapentaenoic acid (EPA), which is one of the nutritionally essential polyunsaturated fatty acids. Therefore, this indigenous isolate exhibits a significant potential as a valuable source of bioactive substances for various bio-industrial applications.

Keywords: Carotenoid pigments; Fatty acids; *Odontella aurita*; Optimal growth condition; Ultrastructure; 18S rDNA

1. Introduction

Microalgae contain various functional substances [1]. Unlike resources such as terrestrial plants and seaweeds, they can be cultured in large quantities, which has the advantage of securing raw materials in a stable manner [2]. Microalgae contain a significant amount of high-value useful substances, including unsaturated fatty acids (such as omega-3 fatty acids), natural pigments (like astaxanthin, lutein, and fucoxanthin), and polysaccharides and oligosaccharides (such as fucoidan, alginic acid, and carrageenan) [3]. It is used in various bio-industries such as the food, health functional food, cosmetics, and pharmaceutical industries [4]. However, despite the high diversity of microalgae, only a few, such as *Chlorella* (Chlorophyta) and *Spirulina* (Cyanobacteria), are used as raw food materials and functional ingredients [5–7]. Since the development of useful materials derived from microalgae has been limited to certain species, there is a strong potential for discovering new sources for biomaterial development in the future.

Diatoms (Bacillariophyta) are the most dominant group of microalgae in marine environments [8]. They are the primary producers in coastal ecosystems [9]. They play a significant role in the biogeochemical cycles of carbon and silicate [10]. Since diatoms have high nutritional value and industrial potential, many studies have been conducted on various diatom species, such as *Cylindrotheca closterium, Nanofrustulum shiloi, Nitzschia laevis, Odontella aurita, Phaeodactylum tricornutum, Skeletonema costatum,* and *Thalassiosira weissflogii* [11–19]. Among them, *O. aurita* is

 doi:10.20944/preprints202309.1848.v1

notable for its elevated concentration of omega-3 fatty acids, particularly eicosapentaenoic acid (EPA) [20]. It also has a high content of functional substances, such as carotenoids, primarily fucoxanthin, and phytosterols [21]. Additionally, *O. aurita* is rich in protein and minerals [18,22,23].

In 2002, the Agence Française de Sécurité Sanitaire des Aliments (AFSSA) granted approval for the consumption of *Odontella aurita*, citing its substantial equivalence to other edible seaweeds that had already been approved under EC Regulation 258/97 [24]. Since then, *O. aurita* has been officially designated as a Novel Food in the European Union (EU) [25]. According to the regulations set by the EU, the entire biomass of *O. aurita* can be utilized in certain food products, subject to maximum content limitations [26]. This particular species is among the limited number of commercially accessible options, even though it has not been officially recognized as safe for consumption by the United States Food and Drug Administration (US FDA) under the Generally Recognized As Safe (GRAS) category [27]. Thus, it possesses the potential to be developed as feed, food and functional material with high value-added properties [28,29]. Additionally, it has been commercially cultivated and utilized in France as a source of human food, dietary supplements, and cosmetic ingredients [30,31].

In the present study, *Odontella aurita* OAOSH22 was isolated and identified from the coastal water of Sonyang-myeon, Yangyang-gun, Gangwon-do, Republic of Korea. Subsequently, a culture consisting of a single algal species was developed. We have identified the recently acquired culture strain through the analysis of its morphology and molecular characteristics. Additionally, we have investigated the optimal culture conditions for this particular algae strain. Furthermore, the investigation examined the composition of fatty acids and carotenoid pigments in order to explore the distinctive properties of these valuable substances, which have potential applications in various industries.

2. Results and Discussion

2.1. Morphological identification of strain OAOSH22

The morphological observations revealed that our isolate exhibited several morphological features that are consistent with the characteristics of the genus *Odontella*. These features include bipolar valves, two elevations at the apices with rimmed ocelli at the summits, two pore occlusion types, a distinct expanded hyaline valve margin with an upturned rim, rimoportulae located in the subcentral position, valvocopula extending beneath the flange, and chain formation [32]. The morphological characteristics of the isolate are outlined in detail below and illustrated in Figure 1. The cells were strongly silicified, with an apical axis of 25–51 μm (n = 16). Numerous small circular or elliptical chloroplasts were observed to be adhered to the cell wall (Figure 1A). The cells typically exhibited a colony formation characterized by a zigzag pattern, with a single horn connecting them, or a linear colony formation with both horns serving as points of connection (Figure 1A). Valves were more or less elliptical (bipolar), with two obtuse horns (elevations) with an ocellus at each pole and a distinct convex area between the horns (Figure 1A, B, F; arrowhead). The valve mantle became increasingly constricted toward the edge and greatly curved outward from the edge again (Figure 1F; arrow). Valves were found to be embedded within the girdle band (Figure 1E, F). Two or more labiate processes (up to 14 observed) with spine-like external tubes were located in the central convex area of each valve (Figure 1D–F). The areolae were arranged radially from the center of the valve (11 in 10 μm, n = 7) and occluded by two types of vela (Figure 1C; arrow and arrowhead). The surface of the valve exhibited a multitude of small spines (Figure 1C, D, F).

Microscopic observations revealed that strain OAOSH22 exhibited the characteristic morphological traits of *O. aurita* (Lyngbye) C.A. Agardh 1832 [32]. The size of *O. aurita* cells exhibits significant variability [33]. Therefore, it can be confused between *O. aurita* and other species that share similar morphological features, such as *O. obtusa* and *Hobaniella longicuris*. *O. obtusa* exhibits shorter and more obtuse horns, displaying greater inflection at the base and a lower elevation at the center of the valve compared to *O. aurita* [34]. *H. longicruris* exhibits elongated and slender horns with minimal curvature at the base in comparison to *O. aurita*. Additionally, it possesses dome-shaped areolae [32].

 doi:10.20944/preprints202309.1848.v1

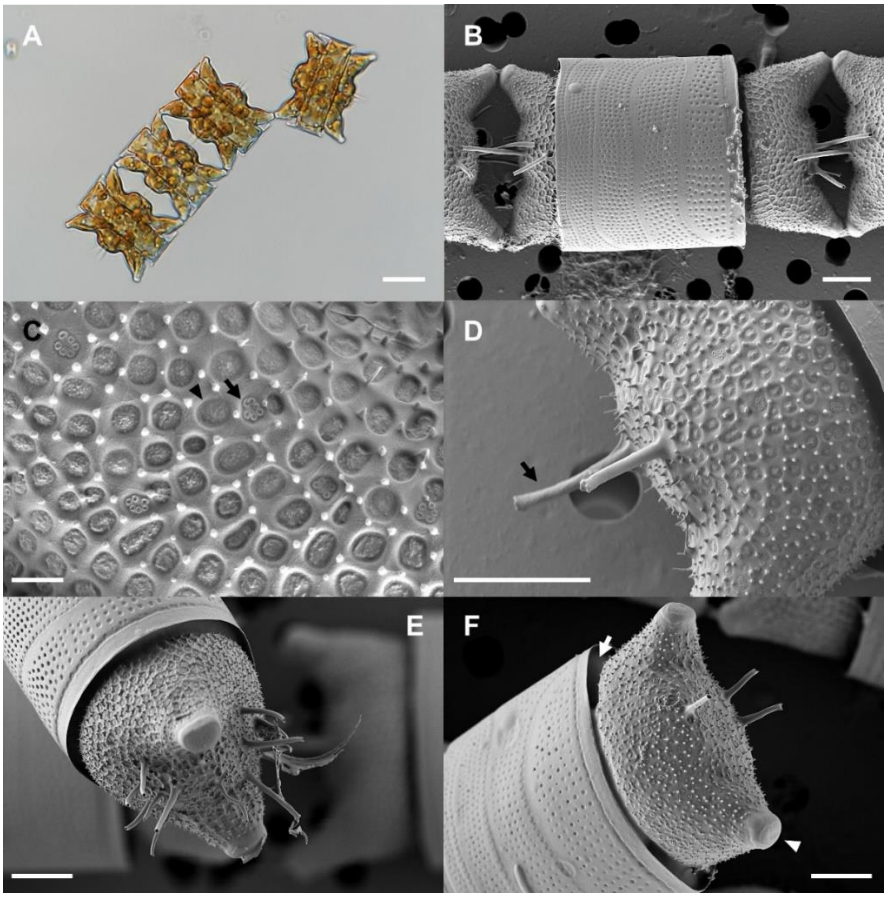

Figure 1. Light and scanning electron microscopy micrographs of *Odontella aurita* OAOSH22. (A) Cells form colonies with one or two horns connected. (B) External whole frustule view. (C) Detail of external areolae occluded by two types of velum (arrow and arrowhead). (D) Detail of external valve central area showing two labiate processes with spine-like external tubes (arrow). (E) the valve with 14 labiate processes. (F) Embedded valve in the girdle band (arrow) and two obtuse horns with ocelli at apices (arrowhead). Scale bars: A = 20 μm, B, D – F = 5 μm and C = 1 μm.

2.2. Molecular identification of strain OAOSH22

The length of the trimmed and assembled 18S rDNA sequences for strain OAOSH22 was determined to be 1,684 base pairs (bp). The sequences obtained as a result of this study have been submitted to GenBank under the accession number OP502635. A BLASTn search was conducted to determine the similarity of the 18S rDNA sequence of strain OAOSH22. The results revealed a high level of identity, with 99.6% similarity (query cover of 100% and E-value of 0), when compared to the 18S rDNA sequence of *Odontella aurita* (MW750334). Based on the BLASTn search results, phylogenetic analyses using Maximum Likelihood (ML) and Bayesian Inference (BI) methods were performed to validate the taxonomic affiliation of strain OAOSH22 within the order Eupodiscales, which encompasses the genus *Odontella*. Strain OAOSH22 exhibited a close relationship with *O. aurita*, supported by robust bootstrap values (ML bootstrap = 98% and BI posterior probabilities = 100%) (Figure 2). Finally, the strain OAOSH22 was identified as *Odontella aurita* through the analysis of morphological characteristics and sequencing data. The strain was deposited in the Korean Collection for Type Cultures (KCTC 15114BP).

Preprints (www.preprints.org) | NOT PEER-REVIEWED | Posted: 30 September 2023 doi:10.20944/preprints202309.1848.v1

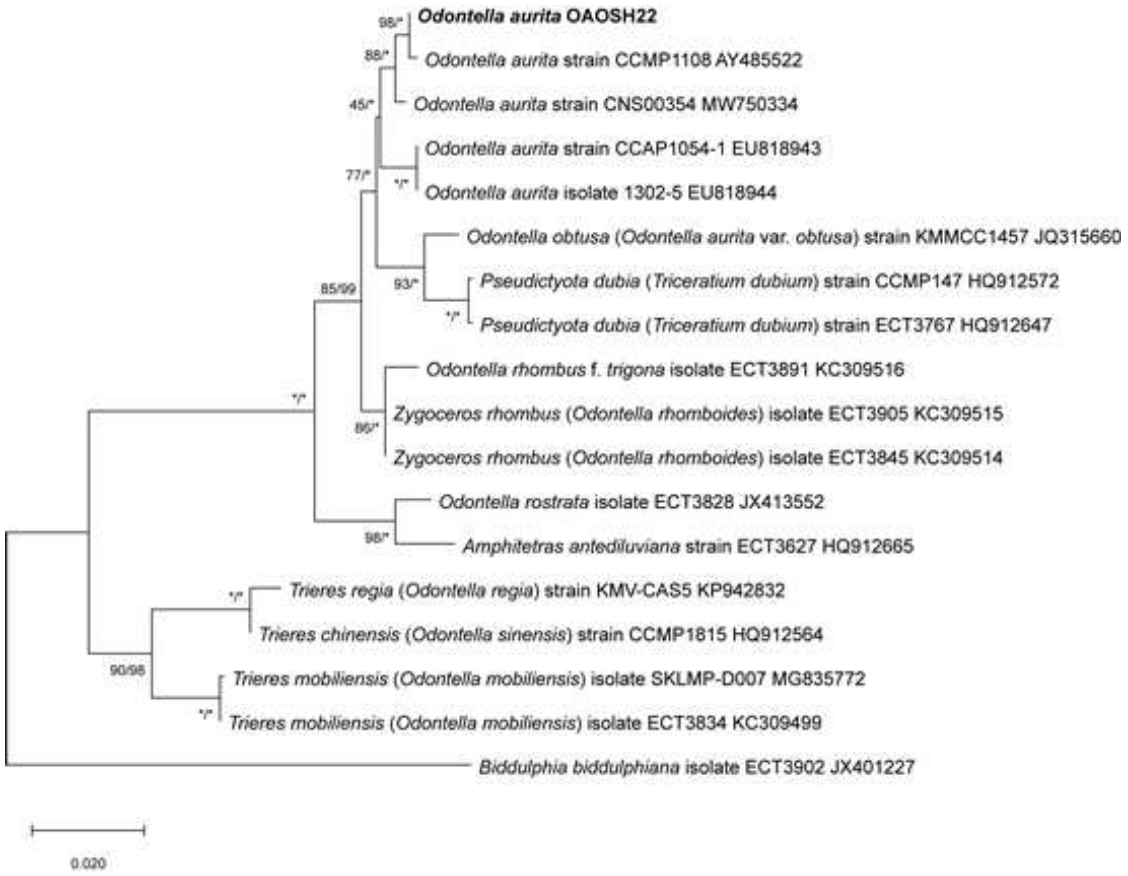

Figure 2. ML and BI Phylogenetic tree of 18S rRNA gene from Eupodiscales species. The values on each node indicate ML bootstrap and Bayesian posterior probabilities (%), respectively. The asterisk indicates 100.

2.3. Optimization of culture conditions for strain OAOSH22

In order to determine the optimal cultivation conditions for *Odontella aurita* OAOSH22, an analysis was conducted to assess the growth response under different conditions of irradiance, temperature, salinity, and nutrient concentration at the laboratory scale (Figs 3 and 4).

The PAM technique is commonly employed for the assessment of parameters associated with the photosynthetic efficiency of microalgae using chlorophyll fluorescence quenching analysis [35]. RLC obtained using PAM technique offer comprehensive insights into the saturation characteristics of electron transport and the overall photosynthetic capacity of microalgal strains [36]. This information can be utilized to ascertain the ideal level of irradiance necessary for the cultivation of a particular type of microalgae [37], and to approximate the highest achievable productivity of the culture when the optimal irradiance is provided [38]. The determination of the light saturation coefficient (E_k), which signifies the point at which photosynthesis reaches saturation, involves the consideration of two factors: the maximum electron transport rate (ETR_{max}) and the initial slope (α) of the RLC. The initial slope of a graph represents the quantum efficiency of photosynthetic electron transport [39]. E_k can be regarded as the ideal irradiance level for the cultivation of microalgal strains [40]. The optimal irradiance (E_k) required to saturate photosynthesis in *O. aurita* OAOSH22 was determined to be 76.5 µmol photons m^{-2} s^{-1} using the rapid light curve method. Furthermore, the ETR_{max} was determined to be 5.29 (Figure 3). The growth of microalgae and the production of biomass are influenced more significantly by suitable irradiance rather than nutrient accessibility, as supported by previous studies [41–43]. High levels of irradiance can lead to photoinhibition, whereas low levels of irradiance can impede growth rates. Various studies have shown that certain microalgae species are capable of attaining their highest growth rates when exposed to irradiances below 100 µmol photons m^{-2} s^{-1} [44]. Additionally, it has been observed that photoinhibition can occur even at irradiance levels ranging from 100 to 200 µmol photons m^{-2} s^{-1}, which is significantly lower than the typical intensity of sunlight [45,46]. The results of this investigation exhibited a resemblance to the

Preprints (www.preprints.org) | NOT PEER-REVIEWED | Posted: 30 September 2023 doi:10.20944/preprints202309.1848.v1

outcomes of previous studies. However, irradiances below 100 µmol photons m^{-2} s^{-1} may be deemed appropriate for laboratory-scale cultivation, as evidenced by the findings of this study. On the contrary, when it comes to large-scale cultivations beyond the pilot scale, it may be necessary to increase the light intensities in order to counteract the self-shading effects [47].

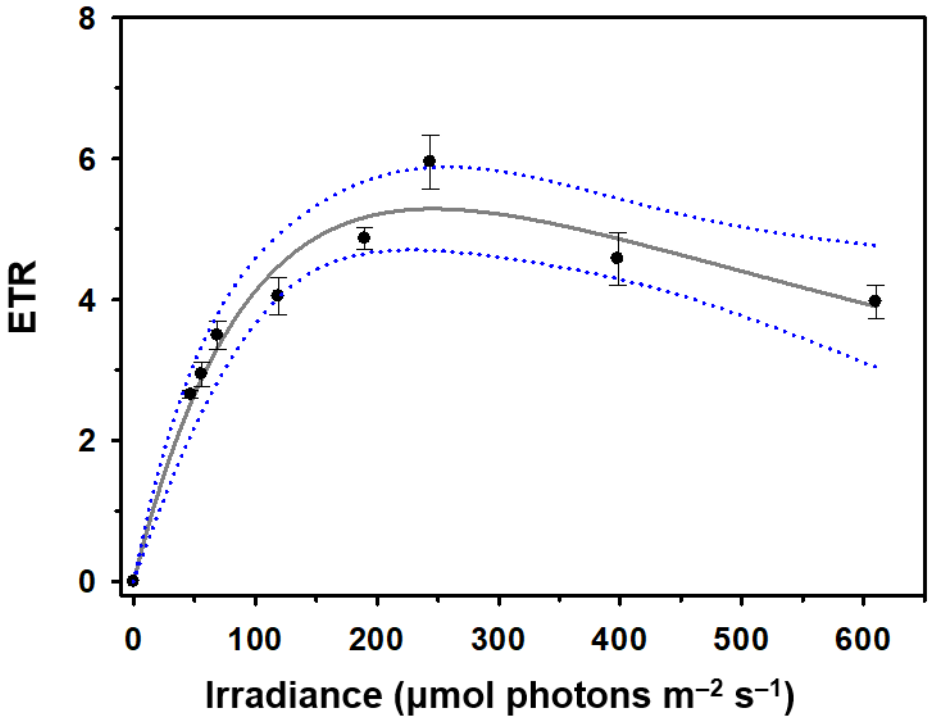

Figure 3. The rapid light-response curve of *Odontella aurita* OAOSH22. Solid lines indicate best fit according to model of Platt et al. [48] and blue dotted lines represent 95% confidence intervals (r^2= 0.96). Symbols and error bars represent the mean ± SE (n = 3).

The growth curves of *O. aurita* OAOSH22 at temperatures of 5, 10, 15, 20, and 25°C are illustrated in Figure 4A. Biomass production attained its maximum value of 138.7 mg L^{-1} following a 9-day incubation period at a temperature of 15°C. However, no growth was observed at both 5°C and 25°C. Temperature is a critical determinant in the growth and development of microalgae [49]. Various aspects are influenced by it, encompassing the growth rate, cell size, biochemical composition, and nutrient requirements [50]. *O. aurita* is a prevalent species that is commonly encountered in temperate regions and exhibits year-round presence. The species under consideration is classified as tychopelagic and is primarily distributed in coastal regions [51]. They primarily inhabit the seafloor during the summer and autumn seasons, and can exert dominance in water columns from late winter to early spring [33,51]. This species was observed to thrive in a temperature range of -1.8 to approximately 26.0°C, with the most favorable temperature for growth reported to be between -1.5 and 6.0°C [52]. Martens [53] conducted a study at the Sylt-Rømø tidal basin, where it was found that a low temperature of -2°C was the main factor responsible for the bloom of *O. aurita*. However, Baars [52] proposed that the species' normal growth is best achieved at temperatures below 20°C. In contrast, Pasquet et al. [54] conducted a study to investigate the impact of temperature on chlorophyll-fluorescent photosynthesis parameters and found that this particular species is capable of tolerating temperatures as high as 28°C.

In order to achieve optimal growth of our strain, it is crucial to consider the salinity of the medium. The growth curves of *O. aurita* OAOSH22 at various salinities (24, 27, 30, 33, and 36 psu) are depicted in Figure 4B. Biomass production reached its peak at 138.2 mg L^{-1} on day 9 of the experiment under a salinity level of 33 psu. Additionally, biomass production exhibited comparable levels within the range of 24 to 30 psu. There is limited existing research on the correlation between growth and salinity levels in *O. aurita*. However, McQuoid [55] found that low salinity levels below 15 psu could

Preprints (www.preprints.org) | NOT PEER-REVIEWED | Posted: 30 September 2023 doi:10.20944/preprints202309.1848.v1

have a detrimental impact on the germination process of *O. aurita*. Therefore, the growth of this species can be significantly reduced by changes in salt levels caused by environmental factors, such as variations in rainfall and drought, during outdoor cultivation.

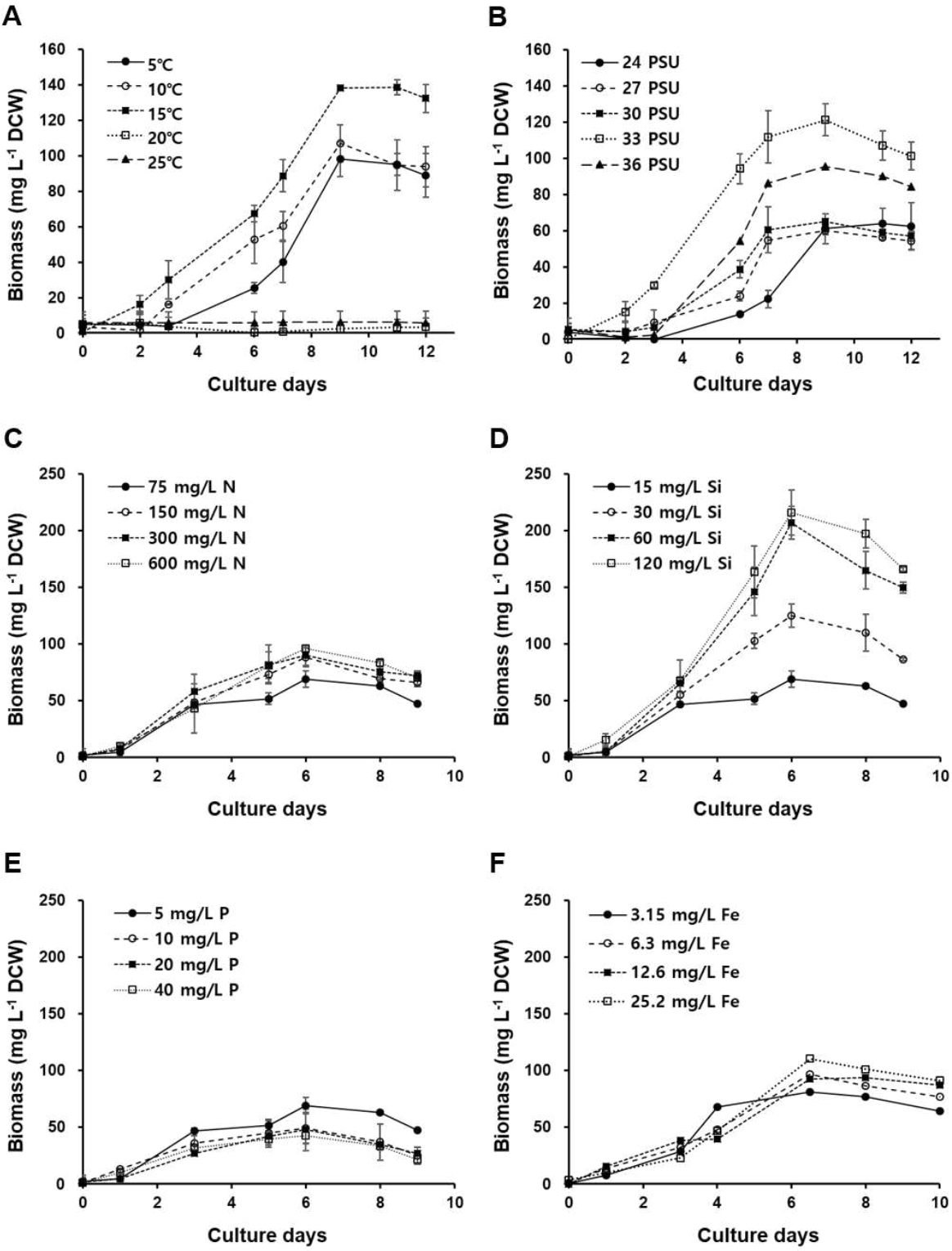

Figure 4. Growth curves of *Odontella aurita* OAOSH22 under different conditions of temperature (a), salinity (b), nitrate (c), silicate (d), phosphate (e), and iron (f). Symbols and error bars represent the mean ± SE (n = 3).

In the present study, the biomass production of *O. aurita* OAOSH22 exhibited a slight increase of approximately 1.2-fold (ca. The biomass production showed slight increase (Figure 4C) when the

concentration of nitrate in the medium was twice enriched (100 mg L^{-1} DCW) compared to the control. However, when the nitrate concentrations were doubled or higher, there was little to no increase in biomass production. Therefore, a concentration of 150 mg N L^{-1}, which is twice the amount of nitrate found in the standard F/2 medium, appears to be adequate for the growth of *O. aurita* OAOSH22. Previous studies have consistently reported a strong correlation between the concentration of nitrate and the biomass of microalgae [56–58]. Similar findings have been observed in studies focusing on *O. aurita* [20,47,59]. However, Xia et al. [60] found that the biomass of *O. aurita* was produced at similar levels (approximately 4 g L^{-1}) under both high (18 mM) and low (6 mM) nitrate concentrations when cultured at 100 μmol photons m^{-2} s^{-1}. Additionally, they observed that biomass production increased by approximately 1.5-fold under high nitrate concentrations compared to low concentrations when cultured at 300 μmol photons m^{-2} s^{-1}. This observation demonstrates that the provision of sufficient nutrients alone may not guarantee optimal growth outcomes, as the fulfillment of basic physical environmental conditions is also crucial in determining growth effects.

In the present study, it was observed that the utilization of a silicate-enriched medium resulted in a significant enhancement in the biomass production of *O. aurita* OAOSH22 (Figure 4D). The growth of *O. aurita* exhibited a positive correlation with the concentration of silicate, as evidenced by the increase in biomass. The maximum biomass of 216 mg L^{-1} was observed on the 6th day of culture when the silicate concentration was 8 times higher than that of the basic F/2 medium. Xia et al. [59] demonstrated that an increase in silicate concentration positively correlated with the biomass production of *O. aurita*. However, contrary to the findings of the present study, no significant difference in biomass production was observed across varying silicate concentrations (27.3–104.2 mg L^{-1}). Silicates play a crucial role as vital nutrients in promoting diatom growth and are indispensable for the development of their cell walls composed of silica [61]. Therefore, the presence of silicates can have a substantial impact on the growth of diatoms [62,63]. When the availability of silicate is limited, a majority of diatoms experience disruptions in their cell cycles during the G1/S or G2/M phases, resulting in thinner frustules [61, 64]. Additionally, the imposition of silicate restriction resulted in a reduction in the fucoxanthin content within *Phaeodactylum tricornutum* [65]. Conversely, it is imperative to appropriately adjust the concentration of silicate based on the target indicator material to be utilized, as research has shown that the restriction of silicate strongly promotes lipid accumulation in diatom cells [66,67].

In the case of phosphate, when the phosphate concentration increased 2–8 times compared to the basic F/2 medium, the biomass production of *O. aurita* decreased 0.6–0.7 times regardless of the concentration, and the additional supply of phosphate negatively affected the growth of *O. aurita* (Figure 4E). Phosphorus comprises a mere 1% of the dry weight of microalgal cells; however, it serves as a significant constraint on microalgal growth in natural environments [50]. However, the impact of phosphorus on the growth of microalgae is comparatively less significant when compared to nitrogen. Additionally, it has been observed that beyond a certain concentration, phosphorus does not contribute to the growth and biomass production of microalgae [68,69]. Lu et al. [70] reported a negative correlation between phosphate concentration and biomass production in their study on *Nitzschia laevis* culture. As a consequence, it appears that providing additional phosphate supply beyond the inherent phosphate concentration present in the F/2 medium is not required for the growth of *O. aurita* OAOSH22.

Iron plays a crucial role in various metabolic processes that regulate photosynthesis through enzymatic reactions. It is a key component of cytochrome b and c, which function as electron transporters in both the photosynthetic and respiratory chain. This involvement of iron positively impacts the growth rate of diatoms [43,71,72]. The study conducted by Sahin et al. [15] demonstrated that *Nanofrustulum shiloi* exhibited 1.3- and 1.1-fold increases in response to an iron-rich environment. Contrarily, the limitation of iron frequently leads to an elevation in the silica composition of diatoms [73]. This, in turn, can cause a reduction in the concentration of silicate in the medium, ultimately resulting in the inhibition of diatom growth. In the present study, *O. aurita* OAOSH22 exhibited no significant variation in biomass production when provided with additional iron supplementation, as compared to the control group (Figure 4F).

2.4. Carotenoid content of strain OAOSH22

Preprints (www.preprints.org) | NOT PEER-REVIEWED | Posted: 30 September 2023 doi:10.20944/preprints202309.1848.v1

The concentration of major carotenoid pigments in *Odontella aurita* OAOSH22 is depicted in Figure 5. Additionally, the LC Chromatogram can be found in Figure S1. The main carotenoid pigment in the isolate obtained in this study was fucoxanthin, with a content of 7.10 ± 0.47 mg g^{-1} DCW. It was also found to contain a small amount of diadinoxanthin (0.98 ± 0.06 mg g^{-1} DCW) and diatoxanthin (1.37 ± 0.04 mg g^{-1} DCW).

The fucoxanthin, a xanthophyll pigment derived from carotenoids, is a naturally occurring pigment. According to Matsuno [74], it is estimated that this particular carotenoid contributes to over 10% of the overall carotenoid production in nature and holds the highest prevalence among carotenoids in marine ecosystems. In the context of fucoxanthin production, it is highly probable that commercially viable microalgae species would include diatoms (Bacillariophyta), Prymnesiales (Haptophyta), and Chrysophyceae (Ochrophyta) [75]. One notable chemotaxonomic characteristic of diatoms is their high concentration of fucoxanthin, which is also found in brown algae [76]. The fucoxanthin content in diatoms is approximately 1–6%, which is over 100 times greater than that found in brown algae [77]. Moreau et al. [28] conducted a study on the anticancer activity of fucoxanthin against bronchopulmonary cancer and epithelial cancer, and reported that *O. aurita* is a significant source of fucoxanthin. Fucoxanthin exhibits health-promoting effects attributed to its potent antioxidant properties [78]. Additionally, it demonstrates anti-obesity, anti-diabetic, anti-cancer, anti-angiogenic, anti-inflammatory, anti-metastatic, and anti-Alzheimer's disease activity [20,79]. Due to its diverse physiological activities, fucoxanthin has found extensive applications in the food, pharmaceutical, and cosmetic industries. It has gained significant attention as a functional material with anti-obesity properties [80,81]. Fucoxanthin has been scientifically proven to possess superior anti-cancer, anti-microbial, and free radical scavenging properties compared to widely used compounds such as β-carotene and astaxanthin [82–85]. It is anticipated that there will be a rise in demand.

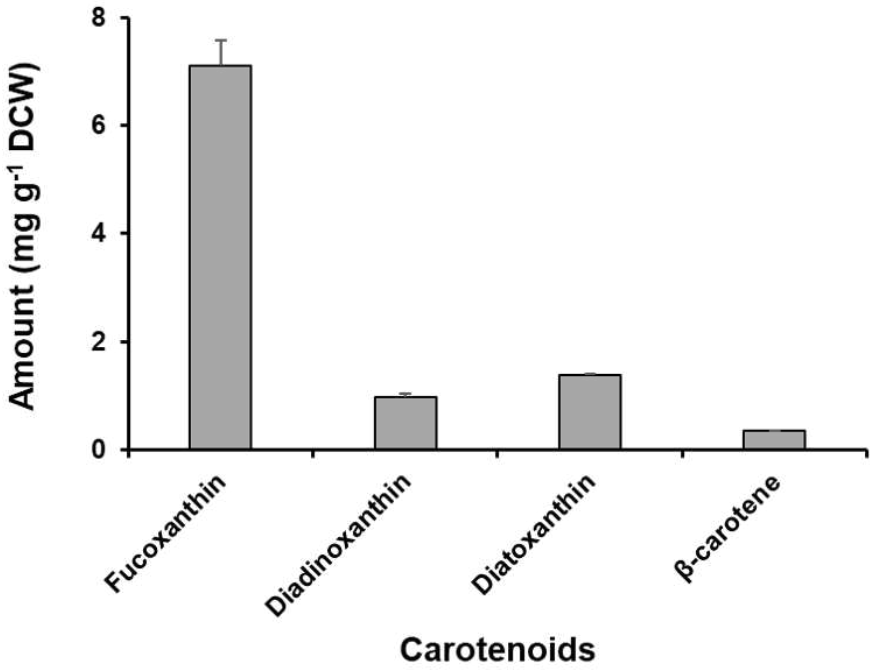

Figure 5. Concentrations of the major carotenoid pigments in *Odontella aurita* OAOSH22.

Xia et al. [59] conducted a study on the fucoxanthin content of *O. aurita* and found that it reached up to 21.7 mg g^{-1} (dry weight). The actual content varied depending on the optimal culture conditions, specifically a light intensity of 100 µmol photons m^{-2} s^{-1} and a nitrate supply of 6 mM. This finding was significant as it represented the highest reported fucoxanthin content in diatoms [86]. Although the fucoxanthin content observed in our study was lower than that reported in previous studies focusing on *O. aurita*, it was found to be comparable to or higher than the levels found in other species such as *Chaetoceros gracilis*, *Cylindrotheca closterium*, *Nitzschia laevis*, and *Phaeodactylum tricornutum*

 doi:10.20944/preprints202309.1848.v1

[69,87,88]. The content of high-value-added substances can vary from strain to strain even in the same species [89], and is influenced by culture conditions such as light intensity [59], temperature [90], salinity [56], nutrient concentration [58], and culture media [91]. For instance, it has been observed that with an increase in light intensity, there is a corresponding increase in microalgal biomass [75]. However, it has also been noted that this increase in light intensity leads to a decrease in fucoxanthin production [92]. Light intensity exceeding 150 μmol photons m^{-2} s^{-1} has been found to induce the synthesis of photoprotective pigments, namely diadinoxanthin and diatoxanthin [93]. Therefore, further investigation into the optimal culture conditions is required in order to enhance the fucoxanthin content.

2.5. Fatty acids composition of strain OAOSH22

The composition of fatty acids in *Odontella aurita* OAOSH22 consisted of saturated fatty acids (SFAs) (42.5%), monounsaturated fatty acids (MUFAs) (37.8%), and polyunsaturated fatty acids (PUFAs) (19.7%). The predominant fatty acids synthesized by this strain were palmitoleic acid (C16:1, 36.4 ± 1.4%), palmitic acid (hexadecanoic acid, C16:0, 25.8 ± 1.0%), eicosapentaenoic acid (EPA, timnodonic acid, C20:5ω3, 17.7 ± 3.3%), and myristic acid (tetradecanoic acid, C14:0, 15.6 ± 1.2%) (Table 1).

Table 1. Fatty acid composition (% total fatty acids) of *Odontella aurita* OAOSH22.

Fatty acids			Amount (mg g^{-1} DCW)	Composition (%)
SFA	**Myristic acid**	C14:0	9.65 ± 0.23	15.61 ± 1.20
	Palmitic acid	C16:0	15.96 ± 0.27	25.76 ± 0.95
	Stearic acid	C18:0	0.68 ± 0.02	1.10 ± 0.09
MUFA	Palmitoleic acid	C16:1n7	22.52 ± 0.36	36.34 ± 1.36
	Oleic acid	C18:1n9	0.93 ± 0.02	1.50 ± 0.05
PUFA	Linoleic acid	C18:2n6 cis	0.75 ± 0.03	1.21 ± 0.01
	Gamma-linolenic acid (GLA)	C18:3n6	0.30 ± 0.03	0.48 ± 0.03
	Arachidonic acid (AA)	C20:4n6	0.22 ± 0.06	0.33 ± 0.09
	Eicosapentaenoic acid (EPA)	C20:5n3	11.07 ± 2.63	17.66 ± 3.28

The distribution of fatty acids exhibits significant variation among different microalgae taxa, as well as within species. Diatoms are commonly known to possess a significant concentration of various fatty acids, including myristic acid (C14:0), palmitic acid (C16:0), palmitoleic acid (C16:1), stearic acid (C18:0), oleic acid (C18:1), and EPA (C20:5ω3) [17,94–97]. These fatty acids play a significant role in various industries such as food, pharmaceuticals, cosmeceuticals, aquaculture, and biofuel [79]. In particular, PUFAs, represented by EPA and docosahexaenoic acid (DHA), have garnered significant interest. PUFAs refers to unsaturated fatty acids containing 18 or more carbon and two or more double bonds [98]. PUFAs, such as omega-3 or omega-6 unsaturated fatty acids, play crucial roles in various physiological processes within the human body. However, these fatty acids are either not naturally synthesized (e.g., linoleic acid and α-linolenic acid) or are synthesized in limited quantities (e.g., EPA, DHA, and arachidonic acid). Consequently, it is necessary to obtain these PUFAs through dietary intake [99]. Among these, EPA offers a range of nutritional and health advantages, including its anti-inflammatory, anti-microbial, anti-cancer, vision and cardiovascular-protective, anti-Parkinsonian syndrome, and anti-Alzheimer's disease effects [20,79].

Odontella aurita is a representative EPA-rich species among microalgae and is known to have an EPA content of more than 20% of the total fatty acid [20,47,54,100–102]. The fatty acid composition of *O. aurita* OAOSH22 was similar to previous studies, but the content of EPA was marginally lower, measuring at 17.7%. Several prior studies have documented that a deficiency of silicate in the growth medium stimulates lipid synthesis and leads to an elevation in EPA levels [65,67,103,104]. Hence, it is postulated that the elevated concentration of silicate in the medium employed in this investigation exerted an adverse impact on the content of EPA.

Currently, the primary source of EPA is derived from oily fish species such as salmon, mackerel, pilchard, herring, and trout [104,105]. However, diatoms present a promising alternative source of EPA, offering the advantage of meeting vegan dietary requirements [86]. In particular, the species *O.*

 doi:10.20944/preprints202309.1848.v1

aurita has already been commercially utilized for food in Europe, suggesting that it holds significant potential in the food and health functional food industries [21,107,108].

Myristic acid, the predominant fatty acid present in this particular strain, serves as a stabilizing agent for a variety of proteins, including those associated with immune system function and anti-cancer properties [109]. Additionally, it finds extensive application in the beauty industry as a fragrance, surfactant, detergent, and emulsifier [110]. Palmitoleic acid has been documented to exhibit antibacterial properties [79], and has recently been suggested as a potential food ingredient for managing complex obesity [111].

3. Materials and Methods

3.1. Sample collection and isolation

A sample was collected from the coastal water at the Osan port (38°5'25.51"N, 128°39'53.36"E) in Yangyang-gun, Gangwon-do, Republic of Korea, on February 16, 2022 by the Survey on Marine Bio-Resources. Cell isolation was conducted utilizing the capillary method employing a Pasteur pipette, while being observed under an Eclipse Ti-U inverted microscope (Nikon, Tokyo, Japan). The isolated cells were subsequently transferred to a cell culture flask (SPL Life Sciences, Pocheon, Korea) containing F/2 medium supplemented with silicate (Sigma Aldrich Co., St. Louis, MO, USA) and a 0.2% antibiotic mixture (Penicillin-streptomycin-neomycin) (Sigma Aldrich Co.). To assess the ability of the isolated strain to grow on a solid medium, the monoculture strain was inoculated onto a 1% agar plate (Bacto Agar, BD Difco Ltd., Detroit, MI, USA) supplemented with F/2 media. Culture strains cultivated in both liquid and solid media were periodically transferred to fresh medium at intervals of three weeks and two months, respectively. The culture strains were then incubated at a temperature of 17℃, a 14:10 h light/dark cycle, and an irradiance of 40 μmol photons m^{-2} s^{-1}.

3.2. Morphological identification

The culture strain was harvested by centrifugation at 2,500 rpm for 5 minutes and mixed with glycerol gelatin (Sigma Aldrich Co.) for mounting on a slide. The mixed sample was placed dropwise on a glass slide and fixed in position with a coverslip. Finally, the margin of the coverslip was sealed with CoverGrip coverslip sealant (Biotium, Hayward, CA, USA). The slide was examined using a Nikon Eclipse Ni light microscope. For scanning electron microscopy (SEM), the cultured strain was fixed in 5% Lugol's solution, filtered through a polycarbonate membrane with a 3 μm pore size and 25 mm diameter (Advantec, Tokyo, Japan), and washed three times with sterile distilled water. The membrane was dehydrated in a graded series of ethanol (10%, 30%, 50%, 70%, 90%, and 100%) and finally dried using tetramethylsilane (Sigma Aldrich Co.). The membrane was mounted on a stub and sputter-coated with gold using an MC1000 ion sputter (Hitachi, Tokyo, Japan). The cells and surface morphology were observed using a high-resolution Zeiss Sigma 500 VP field-emission scanning electron microscope (FE-SEM, Carl Zeiss, Oberkochen, Germany).

3.3. Molecular identification

The culture medium, which contained the strain, was transferred into a 50 mL conical tube and subjected to centrifugation at a speed of 4,000 rpm for a duration of 5 minutes. The supernatant was subsequently removed. Genomic DNA extraction was performed using the DNeasy PowerSoil Pro Kit (Qiagen Inc., Hilden, Germany) according to the manufacturer's instructions. Polymerase chain reaction (PCR) amplification was conducted using the Diatom9F [112] / EukBR [113] primer pairs in order to amplify the 18S rRNA sequence. PCR analysis was conducted following the protocol outlined by An et al. [114]. The PCR product underwent purification using ExoSAP-IT Express PCR Product Cleanup Reagent (Thermo Fisher Scientific, MA, USA) and was subsequently sequenced by Cosmogenetech Co., Ltd. (Seoul, South Korea). The sequence underwent trimming, assembly, and alignment using Geneious Prime v.2022.2.2 (Biomatters Ltd., Auckland, New Zealand). The data set of 18S rRNA sequences was compiled, comprising the genetic sequences of 16 species belonging to the Eupodiscales order, as retrieved from GenBank. *Biddulphia biddulphiana* (JX401227) was utilized as an outgroup. Phylogenetic analyses were performed using maximum likelihood (ML) and Bayesian inference (BI) methods. The Randomized Axelerated Maximum Likelihood (RAxML)

 doi:10.20944/preprints202309.1848.v1

v.8.2.10 [115] and MrBayes version 3.2.7 [116] were employed for the ML and BI analyses, respectively. ML and BI analyses were conducted using the methodologies outlined by An et al. [117].

3.4. Determination of Optimal Culture Conditions

The isolate was cultured under different temperature, salinity, and nutrient conditions to establish the optimal culture conditions. To determine the optimal growth temperature, the temperature experiment compared growth at temperatures ranging from 5 to 25°C. The salinity experiment, on the other hand, compared growth at salinities ranging from 24 to 36‰ using F/2 media containing silicate. These experiments were conducted using a multi-thermo incubator (MTI-202B, Eyela, Tokyo, Japan). In addition, to confirm the growth characteristics based on nutrient concentrations, the isolate was cultured at 17°C using a medium enriched with each nutrient (nitrate, silicate, phosphate, and iron) (Sigma Aldrich Co.). The concentration of each nutrient in the standard F/2 medium was set to the control level. Optimal conditions for each factor were determined through daily growth tests. Detailed experimental conditions for each factor are shown in Table 2.

Table 2. Experimental conditions for determining optimal cultivation conditions for each factor. The minimum condition for each nutrient utilized in the experiments is its presence in a standard F/2 medium.

	Experimental conditions
Temperature (°C)	5, 10, 15, 20, 25
Salinity (psu)	24, 27, 30, 33, 36
Nutrients (mg L^{-1})	
Nitrate ($NaNO_3$)	75, 150, 300, 600
Silicate ($Na_2SiO_3 \bullet 9H_2O$)	15, 30, 60, 120
Phosphate ($NaH_2PO_4 \bullet H_2O$)	5, 10, 20, 40
Iron ($FeCl_3.6H_2O$)	3.15, 6.3, 12.6, 25.2

To determine the optimal growth irradiance, the pulse amplitude modulation (PAM) fluorometry technique was used in this study. 1.5 mL of the culture strain was placed in a 24-well plate (SPL Life Sciences) and dark-adapted for 30 minutes before PAM measurement. Rapid light curve (RLC, ETR versus irradiance curve) was conducted at eight incremental irradiances (47, 56, 69, 119, 190, 244, 398, and 610 µmol photons m^{-2} s^{-1}) of actinic light using the Dual-PAM-100 (Heinz Walz Gmbh, Effeltrich, Germany) equipped with an Optical Unit ED-101US/MD. The light curve was fitted according to the model of Platt et al. [48] to determine the maximum electron transport rate (ETR_{max}), the initial slope of the curve (α), and the irradiance at which ETR saturation occurs (E_k). Data processing was performed following the method described in Ralph and Gademann [36] using SigmaPlot v.12.3 (Systat Software Inc., San Jose, CA, USA).

3.5. Determination of Biomass

The biomass production was calculated based on the equation derived from the calibration curve between chlorophyll fluorescence (with an excitation wavelength of 440 nm and emission of 680 nm) and dry cell weight (DCW) (Figure S2). To obtain a calibration curve of chlorophyll fluorescence versus biomass weight, the chlorophyll fluorescence of five pre-cultures of algae with different cell densities was measured using a microplate reader (Synergy H1, BioTek, Winooski, VT, USA). Each sample was then placed in a pre-weighed tube and centrifuged at 5,000 rpm. After removing the supernatant, the sample was washed once with distilled water to eliminate salt and then centrifuged again. The cell pellet was lyophilized using a benchtop freeze dryer for 24 hours (Freezezone 4.5, Labconco, Kansas City, MO, USA). Finally, the DCW was determined by subtracting the weight of the pre-weighed tube from the total weight of the tube containing the pellet.

3.6. Carotenoids analysis

Carotenoid was analyzed by a slightly modified method of Kang et al. [118] and Baek et al. [119]. To quantify the carotenoids content, algal biomass concentration was calculated using a pre-determined conversion equation mentioned earlier. Subsequently, algal cells were collected by centrifugation at 10,000 rpm for 2 minutes. The supernatant was then removed, and the pigments were extracted from the cells using 100% methanol and algal cells disrupted by ultrasonic water bath

 doi:10.20944/preprints202309.1848.v1

(DAIHAN Scientific, South Korea) for 3 min at 60°C. The resulting supernatant was then filtered through a 0.2 μm PTFE membrane filter (Millipore, Billerica, MA, USA). Carotenoid pigments were analyzed using Agilent 1260 Infinity HPLC system (Agilent, Waldbronn, Germany) equipped with a Spherisorb 5.0 μm ODS1 4.6 × 250 mm cartridge column (Waters, St. Louis, MO, USA) at 40°C. Chromatograms were identified by comparing them to carotenoid standards including fucoxanthin (Sigma Aldrich, USA), diadinoxanthin, diatoxanthin, and β-carotene (DHI, Hørsholm, Denmark) and the concentration of each pigment was calculated using the peak area of the standard pigments.

3.7. Fatty acid analysis

Cells were harvested by centrifugation at 7,000 rpm for fatty acid analysis. After removing as much supernatant as possible, the pellets were lyophilized by freeze-drying at -110°C under a vacuum for 24 hours. Fatty acid extraction was performed following the methods described by Garces and Mancha [120]. The fatty acid composition was analyzed using a 7890A gas chromatograph (Agilent, Wilmington, DE, USA) equipped with a flame ionization detector (280°C, H2 35 mL min^{-1}, air 350 mL min^{-1}, He 30 mL min^{-1}) and a DB-23 column (60 mm × 0.25 mm × 0.25 μm film thickness; Agilent). The initial GC oven temperature was set at 80°C and maintained for 3 minutes. The temperature was ramped at a rate of 15°C min^{-1} to 200°C and held for 8 minutes. It was then ramped at a rate of 1°C min^{-1} to 215°C and held for 8 minutes. After that, it was ramped at a rate of 2°C min^{-1} to 250°C and held for 5 minutes. Finally, it was ramped at a rate of 50°C min^{-1} to 80°C and held for 3 minutes. The sample (2 μl) was injected with a split ratio of 10:1. The injector and detector temperatures were set at 250°C and 280°C, respectively. The identification of fatty acids was performed by comparing their retention time to the retention time of standards (Supelco 37-component FAME mix; Supelco, Bellefonte, PA, USA) and an internal standard (pentadecanoic acid; Sigma Aldrich Co.). Fatty acid analysis was conducted at the National Instrumentation Center for Environmental Management (NICEM) at Seoul National University in the Republic of Korea.

4. Conclusions

In the present study, we acquired an indigenous strain of *Odontella aurita* OAOSH22 and conducted an analysis of its fundamental characteristics and optimal culture conditions. As observed in previous studies on this species, the current isolate also exhibited elevated levels of fucoxanthin and EPA. This particular species has obtained certification and has been utilized as a cosmetic ingredient not only in Korea but also in numerous other countries. Furthermore, it possesses significant potential as a material for food and health functional products. The composition of high-value-added substances is subject to the influence of diverse cultural conditions, including light intensity, temperature, salinity, nutrient concentration, and culture media. Therefore, further investigation is required to enhance the synthesis of valuable compounds and establish optimal conditions for large-scale cultivation in industrial settings.

Supplementary Materials: Supplementary Figure S1: The chromatogram, acquired through High-Performance Liquid Chromatography with Photodiode Array detection (HPLC-PDA), of the carotenoid extract derived from *Odontella aurita* OAOSH22. Supplementary Figure S2 Calibration curve for *Odontella aurita* OAOSH22 based on fluorescence excitation of chlorophyll.

Author Contributions: Conceptualization, Sung Min An; Data curation, Kichul Cho and Nam Seon Kang; Formal analysis, Eun Song Kim and Hyunji Ki; Funding acquisition, Grace Choi; Investigation, Sung Min An, Kichul Cho, Eun Song Kim and Hyunji Ki; Methodology, Sung Min An; Project administration, Grace Choi; Writing – original draft, Sung Min An; Writing – review & editing, Kichul Cho and Nam Seon Kang.

Funding: This research was also supported by the development of useful materials derived from marine microorganisms and microalgae (2023M00600) funded by the National Marine Biodiversity Institute of Korea (MABIK).

Institutional Review Board Statement: Not applicable.

Informed Consent Statement: Not applicable.

Data Availability Statement: Data is contained within the article.

Conflicts of Interest: The authors declare no conflict of interest.

References

1. Dineshbabu, G.; Goswami, G.; Kumar, R.; Sinha, A.; Das, D. Microalgae–nutritious, sustainable aqua- and animal feed source. *J. Funct. Foods* **2019**, *62*, 103545.
2. Nwoba, E.G.; Ogbonna, C.N.; Ishika, T.; Vadiveloo, A. Microalgal pigments: a source of natural food colors. In *Microalgae biotechnology for food, health and high value products*; Alam, M.A., Xu, J.L., Wang, Z., Eds.; Springer: Singapore, 2020 pp. 81–123.
3. Orejuela-Escobar, L.; Gualle, A.; Ochoa-Herrera, V.; Philippidis, G.P. Prospects of microalgae for biomaterial production and environmental applications at biorefineries. *Sustainability* **2021**, *13*, 3063.
4. Chandra, R.; Iqbal, H.M.; Vishal, G.; Lee, H.S.; Nagra, S. Algal biorefinery: a sustainable approach to valorize algal-based biomass towards multiple product recovery. *Bioresour. Technol.* **2019**, *278*, 346–359.
5. Priyadarshani, I.; Rath, B. Commercial and industrial applications of micro algae–A review. J. Algal Biomass Util. **2012**, *3*, 89–100.
6. Andrade, L.M.; Andrade, C.J.; Dias, M.; Nascimento, C.; Mendes, M.A. *Chlorella* and *Spirulina* microalgae as sources of functional foods. Nutraceuticals, and Food Supplements; an Overview. *MOJ food Process Technol.* **2018**, *6*, 45–58.
7. Araújo, R.; Vázquez Calderón, F.; Sánchez López, J.; Azevedo, I.C.; Bruhn, A.; Fluch, S.; Manuel, G.T.; Fatemeh, G.; Tanel, I.; Martial, L.; Micheal, M.M.; Silvio, M.; César, P.; Céline, R.; Tryggvi, S.; Ullmann, J. Current status of the algae production industry in Europe: an emerging sector of the blue bioeconomy. *Front. Mar. Sci.* **2021**, *7*, 626389.
8. Boyd, P.W.; Strzepek, R.; Fu, F.; Hutchins, D.A. Environmental control of open-ocean phytoplankton groups: Now and in the future. *Limnol. Oceanogr.* **2010**, *55*, 1353–1376.
9. Malviya, S.; Scalco, E.; Audic, S.; Vincent, F.; Veluchamy, A.; Poulain, J.; Wincker, P.; Iudicone, D.; Vargas, C.; Bittner, L.; Zingone, A.; Bowler, C. Insights into global diatom distribution and diversity in the world's ocean. *Proc. Natl. Acad. Sci.* **2016**, *133*, E1516–E1525.
10. Dugdale, R.C.; Wilkerson, F.P.; Minas, H.J. The role of silicate pump in driving new production. *Deep Sea Res. I.* **1995**, *42*, 697–719.
11. Rodolfi, L.; Biondi, N.; Guccione, A.; Bassi, N.; D'Ottavio, M.; Arganaraz, G.; Tredici, M.R. Oil and eicosapentaenoic acid production by the diatom *Phaeodactylum tricornutum* cultivated outdoors in Green Wall Panel (GWP®) reactors. *Biotechnol. Bioeng.* **2017**, *114*, 2204–2210.
12. Shah, M.R.; Lutzu, G.A.; Alam, A.; Sarker, P.; Chowdhury, K.; Parsaeimehr, A.; Liang, Y.; Daroch, M. Microalgae in aquafeeds for a sustainable aquaculture industry. *J. Appl. Phycol.* **2018**, *30*, 197–213.
13. Wang, S.; Verma, S.K.; Hakeem Said, I.; Thomsen, L.; Ullrich, M.S.; Kuhnert, N. Changes in the fucoxanthin production and protein profiles in *Cylindrotheca closterium* in response to blue light-emitting diode light. *Microb. Cell Factories* **2018**, *17*, 1–13.
14. Lu, X.; Liu, B.; He, Y.; Guo, B.; Sun, H.; Chen, F. Novel insights into mixotrophic cultivation of *Nitzschia laevis* for co-production of fucoxanthin and eicosapentaenoic acid. *Bioresour. Technol.* **2019**, *294*, 122145.
15. Sahin, M.S.; Khazi, M.I.; Demirel, Z.; Dalay, M.C. Variation in growth, fucoxanthin, fatty acids profile and lipid content of marine diatoms *Nitzschia* sp. and *Nanofrustulum shiloi* in response to nitrogen and iron. *Biocatal. Agric. Biotechnol.* **2019**, *17*, 390–398.
16. Branco-Vieira, M.; San Martin, S.; Agurto, C.; Freitas, M.A.; Martins, A.A.; Mata, T.M.; Caetano, N.S. Biotechnological potential of *Phaeodactylum tricornutum* for biorefinery processes. *Fuel* **2020**, *268*, 117357.
17. Marella, T.K.; Tiwari, A. Marine diatom *Thalassiosira weissflogii* based biorefinery for co-production of eicosapentaenoic acid and fucoxanthin. *Bioresour. Technol.* **2020**, *307*, 123245.
18. Stiefvatter, L.; Lehnert, K.; Frick, K.; Montoya-Arroyo, A.; Frank, J.; Vetter, W.; Schmid-Staiger, U.; Bischoff, S.C. Oral Bioavailability of Omega-3 Fatty Acids and Carotenoids from the Microalgae *Phaeodactylum tricornutum* in Healthy Young Adults. *Mar. Drugs* **2021**, *19*, 700.
19. Zhang, H.; Gong, P.; Cai, Q.; Zhang, C.; Gao, B. Maximizing fucoxanthin production in *Odontella aurita* by optimizing the ratio of red and blue light-emitting diodes in an auto-controlled internally illuminated photobioreactor. *Bioresour. Technol.* **2022**, *344*, 126260.
20. Xia, S.; Gao, B.; Fu, J.; Xiong, J.; Zhang, C. Production of fucoxanthin, chrysolaminarin, and eicosapentaenoic acid by *Odontella aurita* under different nitrogen supply regimes. *J. Biosci. Bioeng.* **2018**, *126*, 723–729.
21. Haimeur, A.; Ulmann, L.; Mimouni, V.; Guéno, F.; Pineau-Vincent, F.; Meskini, N.; Tremblin, G. The role of *Odontella aurita*, a marine diatom rich in EPA, as a dietary supplement in dyslipidemia, platelet function and oxidative stress in high-fat fed rats. *Lipids Health Dis.* **2012**, *11*, 1–13.
22. Bernaerts, T.M.; Gheysen, L.; Kyomugasho, C.; Kermani, Z.J.; Vandionant, S.; Foubert, I.; Hendrickx, M.E.; Van Loey, A.M. Comparison of microalgal biomasses as functional food ingredients: Focus on the composition of cell wall related polysaccharides. *Algal Res.* **2018**, *32*, 150–161.
23. Terriente-Palacios, C.; Castellari, M. Levels of taurine, hypotaurine and homotaurine, and amino acids profiles in selected commercial seaweeds, microalgae, and algae-enriched food products. *Food Chem.* **2022**, *368*, 130770.

24. Avis de l'Agence française de sécurité sanitaire des aliments relatif à la demande d'évaluation de la démonstration de l'équivalence en substance d'une microalgue *Odontella aurita* avec des algues autorisées (AFSSA Saisine no. 2001-SA-0082). Available online: https://www.anses.fr/fr/system/files/AAAT2001sa0082.pdf (accessed 12 Sep 2023).
25. Summary of notifications received by the Commission until 31 December 2004 pursuant to Article 5 of Regulation (EC) No 258/97 of the European Parliament and of the Council (2005/C 208/2). Available online: https://eur-lex.europa.eu/legal-content/EN/TXT/?uri=CELEX%3A52005XC0825%2801%29&qid=1674696011584 (accessed 12 Sep 2023).
26. Commission Implementing Regulation (EU) 2017/2470 of 20 December 2017 establishing the Union list of novel foods in accordance with Regulation (EU) 2015/2283 of the European Parliament and of the Council on novel foods. Available online: https://eur-lex.europa.eu/eli/reg_impl/2017/2470/oj (accessed 12 Sep 2023).
27. US Food and Drug Administration. GRAS Notices. Available online: https://www.cfsanappsexternal.fda.gov/scripts/fdcc/cfc/XMLService.cfc?method=downloadxls&set=GRASNotices (accessed 12 Sep 2023).
28. Moreau, D.; Tomasoni, C.; Jacquot, C.; Kaas, R.; Le Guedes, R.; Cadoret, J.P.; Muller-Feuga, A.; Kontiza, I.; Viagas, C.; Roussis, V.; Roussakis, C. Cultivated microalgae and carotenoid fucoxanthin from *Odontella aurita* as potent anti-proliferative agents in bronchopulmonary and epithelial cell lines. *Environ. Toxicol. Pharmacol.* **2006**, *22*, 97–103.
29. Zhao, W.; Yao, R.; He, X.S.; Liao, Z.H.; Liu, Y.T.; Gao, B.Y.; Zhang, C.W.; Niu, J. Beneficial contribution of the microalga *Odontella aurita* to the growth, immune response, antioxidant capacity, and hepatic health of juvenile golden pompano (*Trachinotus ovatus*). *Aquaculture* **2022**, *555*, 738206.
30. Mourelle, M.L.; Gómez, C.P.; Legido, J.L. The potential use of marine microalgae and cyanobacteria in cosmetics and thalassotherapy. *Cosmetics* **2017**, *4*, 46.
31. Fleurence, J. *Microalgae: From Future Food to Cellular Factory*; John Wiley & Sons: Hoboken, NJ, USA, 2021; pp. 13–89.
32. Sims, P.A.; Williams, D.M.; Ashworth, M. Examination of type specimens for the genera *Odontella* and *Zygoceros* (Bacillariophyceae) with evidence for the new family Odontellaceae and a description of three new genera. *Phytotaxa* **2018**, *382*, 1–56.
33. Kraberg, A.; Baumann, M.; Dürselen, C.D. *Coastal phytoplankton: photo guide for Northern European seas*; Verlag Dr. Friedrich Pfeil: München, Germany, 2010; pp. 96–97.
34. Lavigne, A.S.; Sunesen, I.; Sar, E.A. Morphological, taxonomic and nomenclatural analysis of species of *Odontella, Trieres* and *Zygoceros* (Triceratiaceae, Bacillariophyta) from Anegada Bay (Province of Buenos Aires, Argentina). *Diatom Res.* **2015**, *30*, 307–331.
35. Elisabeth, B.; Rayen, F.; Behnam, T. Microalgae culture quality indicators: a review. *Crit. Rev. Biotechnol.* **2021**, 41, 457–473.
36. Ralph, P.J.; Gademann, R. Rapid light curves: a powerful tool to assess photosynthetic activity. *Aquat. Bot.* **2005**, *82*, 222–237.
37. Bhola, V.; Desikan, R.; Santosh, S.K.; Subburamu, K.; Sanniyasi, E.; Bux, F. Effects of parameters affecting biomass yield and thermal behaviour of *Chlorella vulgaris*. *J. Biosci. Bioeng.* **2011**, *111*, 377–382.
38. Barceló Villalobos, M. Optimización de la producción de microalgas en reactores abiertos de escala industrial. Ph.D. Thesis, University of Almería, Spain, 2020.
39. Consalvey, M.; Perkins, R.G.; Paterson, D.M.; Underwood, G.J. PAM fluorescence: a beginners guide for benthic diatomists. *Diatom Res.* **2005**, *20*, 1–22.
40. Malapascua, J.R.; Jerez, C.G.; Sergejevová, M.; Figueroa, F.L.; Masojídek, J. Photosynthesis monitoring to optimize growth of microalgal mass cultures: application of chlorophyll fluorescence techniques. *Aquat. Biol.* **2014**, *22*, 123–140.
41. Hempel, N.; Petrick, I.; Behrendt, F. Biomass productivity and productivity of fatty acids and amino acids of microalgae strains as key characteristics of suitability for biodiesel production. *J. appl. phycol.* **2012**, *24*, 1407–1418.
42. He, Q.; Yang, H.; Wu, L.; Hu, C. Effect of light intensity on physiological changes, carbon allocation and neutral lipid accumulation in oleaginous microalgae. *Bioresour. Technol.* **2015**, *191*, 219–228.
43. Moreno, C.M.; Lin, Y.; Davies, S.; Monbureau, E.; Cassar, N.; Marchetti, A. Examination of gene repertoires and physiological responses to iron and light limitation in Southern Ocean diatoms. *Polar Biol.* **2018**, *41*, 679–696.
44. Richardson, K.; Beardall, J.; Raven, J.A. Adaptation of unicellular algae to irradiance. an analysis of strategies. *New Phytol.* 1983, 93, 157–191.
45. Kirk, J.T.O. *Light and Photosynthesis in Aquatic Ecosystems*, 2nd ed.; Cambridge University Press: Cambridge, UK, 1994; 509 p.
46. Masojídek, J.; Koblížek, M.; Torzillo, G. Photosynthesis in Microalgae. In *Handbook of Microalgal Culture: Biotechnology and Applied Phycology*; Richmond, A. Ed.; Blackwell Science Ltd.: Oxford, UK, 2004; pp. 20–39.

47. Roleda, M.Y.; Slocombe, S.P.; Leakey, R.J.; Day, J.G.; Bell, E.M.; Stanley, M.S. Effects of temperature and nutrient regimes on biomass and lipid production by six oleaginous microalgae in batch culture employing a two-phase cultivation strategy. *Bioresour. Technol.* **2013**, *129*, 439–449.
48. Platt, T.G.C.L.; Gallegos, C.L.; Harrison, W.G. Photoinhibition of photosynthesis in natural assemblages of marine phytoplankton. *J. Mar. Res.* **1980**, *38*, 687–701.
49. Ras, M.; Steyer, J.P.; Bernard, O. Temperature effect on microalgae: a crucial factor for outdoor production. *Rev. Environ. Sci. Biotechnol.* **2013**, *12*, 153–164.
50. Khaw, Y.S.; Yusoff, F.M.; Tan, H.T.; Noor Mazli, N.A.I.; Nazarudin, M.F.; Shaharuddin, N.A.; Omar, A.R.; Takahashi, K. Fucoxanthin Production of Microalgae under Different Culture Factors: A Systematic Review. *Mar. Drugs* **2022**, *20*, 592.
51. Hoppenrath, M.; Elbrächter, M.; Drebes, G. *Marine phytoplankton Selected Microphytoplankton Species from the North Sea Around Helgoland and Sylt.* Schweizerbart Sche Vlgsb.: Stuttgart, Germany, 2009; 264 p.
52. Baars, J.W.M. Autecological investigations on marine diatoms. 4: *Biddulphia aurita* (Lyngb.) Brebisson et Godey—A succession of spring diatoms. *Hydrobiol. Bull.* **1985**, *19*, 109–116.
53. Martens, P. Effects of the severe winter 1995/96 on the biological oceanography of the Sylt-Rømø tidal basin. *Helgol. Mar. Res.* **2001**, *55*, 166–169.
54. Pasquet, V.; Ulmann, L.; Mimouni, V.; Guihéneuf, F.; Jacquette, B.; Morant-Manceau, A.; Tremblin, G. Fatty acids profile and temperature in the cultured marine diatom *Odontella aurita*. *J. Appl. Phycol.* **2014**, *26*, 2265–2271.
55. McQuoid, M.R. Influence of salinity on seasonal germination of resting stages and composition of microplankton on the Swedish west coast. *Mar. Ecol. Prog. Ser.* **2005**, *289*, 151–163.
56. Wang, H.; Zhang, Y.; Chen, L.; Cheng, W.; Liu, T. Combined Production of Fucoxanthin and EPA from Two Diatom Strains *Phaeodactylum tricornutum* and *Cylindrotheca fusiformis* Cultures. *Bioprocess Biosyst. Eng.* **2018**, *41*, 1061–1071.
57. Zarrinmehr, M.J.; Farhadian, O.; Heyrati, F.P.; Keramat, J.; Koutra, E.; Kornaros, M.; Daneshvar, E. (2019) Effect of nitrogen concentration on the growth rate and biochemical composition of the microalga, *Isochrysis galbana*. *Egypt. J. Aquat. Res.* **2019**, *46*, 153–158.
58. Premaratne, M.; Liyanaarachchi, V.C.; Nimarshana, P.H.V.; Ariyadasa, T.U.; Malik, A.; Attalage, R.A. Co-Production of Fucoxanthin, Docosahexaenoic Acid (DHA) and Bioethanol from the Marine Microalga *Tisochrysis lutea*. *Biochem. Eng. J.* **2021**, *176*, 108160.
59. Xia, S.; Wan, L.; Li, A.; Sang, M.; Zhang, C. Effects of nutrients and light intensity on the growth and biochemical composition of a marine microalga *Odontella aurita*. *Chin. J. Oceanol. Limnol.* **2013**, *31*, 1163–1173.
60. Xia, S.; Wang, K.; Wan, L.; Li, A.; Hu, Q.; Zhang, C. Production, characterization, and antioxidant activity of fucoxanthin from the marine diatom *Odontella aurita*. *Mar. Drugs* **2013**, *11*, 2667–2681.
61. Martin-Jézéquel, V.; Hildebrand, M.; Brzezinski, M.A. Silicon metabolism in diatoms: implications for growth. *J. Phycol.* **2000**, *36*, 821–840.
62. Mao, X.; Chen, S.H.Y.; Lu, X.; Yu, J.; Liu, B. High silicate concentration facilitates fucoxanthin and eicosapentaenoic acid (EPA) production under heterotrophic condition in the marine diatom *Nitzschia laevis*. *Algal Res.* **2020**, *52*, 102086.
63. Couto, C.; Hernández, C.P.; Alves Sobrinho, R.C.M.; Mendes, C.R.B.; Roselet, F.; Abreu, P.C. Optimization of a low-cost fertilizer-based medium for large-scale cultivation of the coastal diatom *Conticribra weissflogii* using response surface methodology and its effects on biomass composition. *J. Appl. Phycol.* **2021**, *33*, 2767–2781.
64. Huysman, M.J.; Vyverman, W.; De Veylder, L. Molecular regulation of the diatom cell cycle. *J. Exp. Bot.* **2014**, *65*, 2573–2584.
65. Patel, A.; Matsakas, L.; Hrůzová, K.; Rova, U.; Christakopoulos, P. Biosynthesis of nutraceutical fatty acids by the oleaginous marine microalgae *Phaeodactylum tricornutum* utilizing hydrolysates from organosolv-pretreated birch and spruce biomass. *Mar. Drugs* **2019**, *17*, 119.
66. Hildebrand, M.; Davis, A.K.; Smith, S.R.; Traller, J.C.; Abbriano, R. The place of diatoms in the biofuels industry. *Biofuels* **2012**, *3*, 221–240.
67. Jung, J.H.; Sirisuk, P.; Ra, C.H.; Kim, J.M.; Jeong, G.T.; Kim, S.K. Effects of green LED light and three stresses on biomass and lipid accumulation with two-phase culture of microalgae. *Process Biochem.* **2019**, *77*, 93–99.
68. Yang, M.; Zhao, W.; Xie, X. Effects of nitrogen, phosphorus, iron and silicon on growth of five species of marine benthic diatoms. *Acta Ecol. Sin.* **2014**, *34*, 311–319.
69. Sun, P.; Wong, C.C.; Li, Y.; He, Y.; Mao, X.; Wu, T.; Ren, Y.; Chen, F. A Novel Strategy for Isolation and Purification of Fucoxanthinol and Fucoxanthin from the Diatom *Nitzschia laevis*. *Food Chem.* **2019**, *277*, 566–572.
70. Lu, X.; Sun, H.; Zhao, W.; Cheng, K.W.; Chen, F.; Liu, B. A hetero-photoautotrophic two-stage cultivation process for production of fucoxanthin by the marine diatom *Nitzschia laevis*. *Mar. Drugs* **2018**, *16*, 219.

71. Kosakowska, A.; Lewandowska, J.; Stoń, J.; Burkiewicz, K. Qualitative and quantitative composition of pigments in *Phaeodactylum tricornutum* (Bacillariophyceae) stressed by iron. *BioMetals* **2004**, *17*, 45–52.
72. Behrenfeld, M.J.; Milligan, A.J. Photophysiological expressions of iron stress in phytoplankton. *Annu. Rev. Mar. Sci.* **2013**, *5*, 217–246.
73. Wilken, S.; Hoffmann, B.; Hersch, N.; Kirchgessner, N.; Dieluweit, S.; Rubner, W.; Hoffmann, L.J.; Merkel, R.; Peeken, I. Diatom frustules show increased mechanical strength and altered valve morphology under iron limitation. *Limnol. Oceanogr.* **2011**, *56*, 1399–1410.
74. Matsuno, T. Aquatic animal carotenoids. *Fish. Sci.* **2001**, *67*, 771–783.
75. Leong, Y.K.; Chen, C.Y.; Varjani, S.; Chang, J.S. Producing fucoxanthin from algae–Recent advances in cultivation strategies and downstream processing. *Bioresour. Technol*. **2022**, *344*, 126170.
76. Peng, J.; Yuan, J.P.; Wu, C.F.; Wang, J.H. Fucoxanthin, a marine carotenoid present in brown seaweeds and diatoms: metabolism and bioactivities relevant to human health. *Mar. Drugs* **2011**, *9*, 1806–1828.
77. Yang, R.; Wei, D.; Xie, J. Diatoms as cell factories for high-value products: chrysolaminarin, eicosapentaenoic acid, and fucoxanthin. *Crit. Rev. Biotechnol.* **2020**, *40*, 993–1009.
78. Maeda, H.; Fukuda, S.; Izumi, H.; Saga, N. Anti-oxidant and fucoxanthin contents of brown alga Ishimozuku (*Sphaerotrichia divaricata*) from the West Coast of Aomori, Japan. *Mar. Drugs* **2018**, *16*, 255.
79. Mal, N.; Srivastava, K.; Sharma, Y.; Singh, M.; Rao, K.M.; Enamala, M.K.; Chandrasekhar, K.; Chavali, M. Facets of diatom biology and their potential applications. *Biomass Convers. Biorefin.* **2022**, *12*, 1959–1975.
80. Matsumoto, M.; Hosokawa, M.; Matsukawa, N.; Hagio, M.; Shinoki, A.; Nishimukai, M.; Miyashita, K.; Yajima, T.; Hara, H. Suppressive effects of the marine carotenoids, fucoxanthin and fucoxanthinol on triglyceride absorption in lymph duct-cannulated rats. *Eur. J. Nutr.* **2010**, *49*, 243–249.
81. Gammone, M.A.; D'Orazio, N. Anti-obesity activity of the marine carotenoid fucoxanthin. *Mar. Drugs* **2015**, *13*, 2196–2214.
82. Neumann, U.; Derwenskus, F.; Flaiz Flister, V.; Schmid-Staiger, U.; Hirth, T.; Bischoff, S.C. Fucoxanthin, a carotenoid derived from *Phaeodactylum tricornutum* exerts antiproliferative and antioxidant activities in vitro. *Antioxidants* **2019**, *8*, 183.
83. Yusoff, F.M.; Banerjee, S.; Nagao, N.; Imaizumi, Y.; Shariff, M.; Toda, T. (2020) Use of microalgae pigments in aquaculture. In *Pigments from Microalgae Handbook*; Jacob-Lopes, E., Queiroz, M.I., Zepka, L.Q., Fds.; Springer: Cham, Switzerland, 2020; pp. 471-513.
84. Karpiński, T.M.; Ożarowski, M.; Alam, R.; Łochyńska, M.; Stasiewicz, M. What Do We Know about Antimicrobial Activity of Astaxanthin and Fucoxanthin?. *Mar. Drugs* **2021**, *20*, 36.
85. Lourenço-Lopes, C.; Fraga-Corral, M.; Jimenez-Lopez, C.; Carpena, M.; Pereira, A.G.; García-Oliveira, P.; Prieto, M.A.; Simal-Gandara, J. Biological action mechanisms of fucoxanthin extracted from algae for application in food and cosmetic industries. *Trends in Food Sci. Technol.* **2021**, *117*, 163–181.
86. Marella, T.K.; López-Pacheco, I.Y.; Parra-Saldívar, R.; Dixit, S.; Tiwari, A. (2020) Wealth from waste: Diatoms as tools for phycoremediation of wastewater and for obtaining value from the biomass. *Sci. Total Environ.* **2020**, *724*, 137960.
87. Pasquet, V.; Chérouvrier, J.R.; Farhat, F.; Thiéry, V.; Piot, J.M.; Bérard, J.B.; Kaas, R.; Serive, B.; Patrice, T.; Cadoret, J.P.; Picot, L. Study on the microalgal pigments extraction process: Performance of microwave assisted extraction. *Process Biochem.* **2011**, *46*, 59–67.
88. Kim, S.M.; Kang, S.W.; Kwon, O.N.; Chung, D.; Pan, C.H. Fucoxanthin as a major carotenoid in *Isochrysis* aff. *galbana*: Characterization of extraction for commercial application. *J. Korean Soc. Appl. Biol. Chem.* **2012**, *55*, 477–483.
89. Shifrin, N.S.; Chisholm, S.W. Phytoplankton lipids: Interspecific differences and effects of nitrate, silicate and light-dark cycles. *J. Phycol.* **1981**, *17*, 374–384.
90. Gao, F.; Teles, I.; Wijffels, R.H.; Barbosa, M.J. Process optimization of fucoxanthin production with *Tisochrysis lutea*. *Bioresour. Technol.* **2020**, *315*, 123894.
91. Tokushima, H.; Inoue-Kashino, N.; Nakazato, Y.; Masuda, A.; Ifuku, K.; Kashino, Y. Advantageous characteristics of the diatom *Chaetoceros gracilis* as a sustainable biofuel producer. *Biotechnol. Biofuels* **2016**, *9*, 1–19.
92. Li, Y.; Sun, H.; Wu, T.; Fu, Y.; He, Y.; Mao, X. Storage Carbon Metabolism of *Isochrysis zhangjiangensis* under Different Light Intensities and Its Application for Co-Production of Fucoxanthin and Stearidonic Acid. *Bioresour. Technol.* **2019**, *282*, 94–102.
93. Lavaud, J.; Rousseau, B.; van Gorkom, H.J.; Etienne, A.L. Influence of the Diadinoxanthin Pool Size on Photoprotection in the Marine Planktonic Diatom *Phaeodactylum tricornutum*. *Plant Physiol.* **2002**, *129*, 1398–1406.
94. Nichols, P.D.; Palmisano, A.C.; Smith, G.A.; White, D.C. Lipids of the Antarctic sea ice diatom *Nitzschia cylindrus*. *Phytochemistry* **1986**, *25*, 1649–1653.
95. Dijkman, N.A.; Kromkamp, J.C. Phospholipid-derived fatty acids as chemotaxonomic markers for phytoplankton: application for inferring phytoplankton composition. *Mar. Ecol. Prog. Ser.* **2006**, *324*, 113–125.

96. Taipale, S.; Strandberg, U.; Peltomaa, E.; Galloway, A.W.; Ojala, A.; Brett, M.T. Fatty acid composition as biomarkers of freshwater microalgae: analysis of 37 strains of microalgae in 22 genera and in seven classes. *Aquat. Microb. Ecol.* **2013**, *71*, 165–178.
97. Artamonova, E.Y.; Svenning, J.B.; Vasskog, T.; Hansen, E.; Eilertsen, H.C. Analysis of phospholipids and neutral lipids in three common northern cold water diatoms: *Coscinodiscus concinnus*, *Porosira glacialis*, and *Chaetoceros socialis* by ultra-high performance liquid chromatography-mass spectrometry, *J. Appl. Phycol.* **2017**, *29*, 1241e1249.
98. Kapoor, B.; Kapoor, D.; Gautam, S.; Singh, R.; Bhardwaj, S. Dietary polyunsaturated fatty acids (PUFAs): Uses and potential health benefits. *Curr. Nutr. Rep.* **2021**, *10*, 232–242.
99. Mariamenatu, A.H.; Abdu, E.M. Overconsumption of omega-6 polyunsaturated fatty acids (PUFAs) versus deficiency of omega-3 PUFAs in modern-day diets: the disturbing factor for their "balanced antagonistic metabolic functions" in the human body. *J. Lipids* **2021**, *2021*, 8848161.
100. Orcutt, D.M.; Patterson, G.W. Sterol, fatty acid and elemental composition of diatoms grown in chemically defined media. *Comp. Biochem. Physiol. B* **1975**, *50*, 579–583.
101. Brand, J.P. Simultaneous culture in pilot tanks of the macroalga *Chondrus crispus* and the microalgae *Odontella aurita* producing EPA. In *Marine Microorganisms for Industry*; Le Gal, Y., Muller-Feuga, A. Eds.; Editions Ifremer: Plouzané, France, 1998; pp. 39–47.
102. Guihéneuf, F.; Fouqueray, M.; Mimouni, V.; Ulmann, L.; Jacquette, B.; Tremblin, G. Effect of UV stress on the fatty acid and lipid class composition in two marine microalgae *Pavlova lutheri* (Pavlovophyceae) and *Odontella aurita* (Bacillariophyceae). *J. appl. Phycol.* **2010**, *22*, 629–638.
103. Roessler, P.G. Effects of silicon deficiency on lipid composition and metabolism in the diatom *Cyclotella cryptica*. *J. Phycol.* **1988**, *24*, 394–400.
104. Hu, Q.; Sommerfeld, M.; Jarvis, E.; Ghirardi, M.; Posewitz, M.; Seibert, M.; Darzins, A. Microalgal triacylglycerols as feedstocks for biofuel production: perspectives and advances. *Plant J.* **2008**, *54*, 621–639.
105. Pike, I.H.; Jackson, A. Fish oil: production and use now and in the future. *Lipid Technol.* **2010**, *22*, 59–61.
106. Wall, R.; Ross, R.P.; Fitzgerald, G.F.; Stanton, C. Fatty acids from fish: the anti-inflammatory potential of long-chain omega-3 fatty acids. *Nutr. Rev.* **2010**, *68*, 280–289.
107. Mimouni, V.; Ulmann, L.; Pasquet, V.; Mathieu, M.; Picot, L.; Bougaran, G.; Cadoret, J.P.; Morant-Manceau, A.; Schoefs, B. The potential of microalgae for the production of bioactive molecules of pharmaceutical interest. *Curr. Pharm. Biotechnol.* **2012**, *13*, 2733–2750.
108. Buono, S.; Langellotti, A.L.; Martello, A.; Rinna, F.; Fogliano, V. Functional ingredients from microalgae. *Food Funct.* **2014**, *5*, 1669–1685.
109. Vidhyalakshmi, R.; Nachiyar, C.V.; Kumar, G.N.; Sunkar, S.; Badsha, I. Production, characterization and emulsifying property of exopolysaccharide produced by marine isolate of *Pseudomonas fluorescens*. *Biocatal. Agric. Biotechnol.* **2018**, *16*, 320–325.
110. Pushpabharathi, N.; Jayalakshmi, M.; Amudha, P.; Vanitha, V. Identification of bioactive compounds in *Cymodocea serrulata*-a seagrass by gas chromatography–mass spectroscopy. *Asian J. Pharm. Clin. Res.* **2018**, *11*, 317–320.
111. Tovar, R.; Gavito, A.L.; Vargas, A.; Soverchia, L.; Hernandez-Folgado, L.; Jagerovic, N.; Baixeras, E.; Ciccocioppo, R.; de Fonseca, F.R.; Decara, J. Palmitoleoylethanolamide is an efficient anti-obesity endogenous compound: comparison with oleylethanolamide in diet-induced obesity. *Nutrients* **2021**, *13*, 2589.
112. Lynch, E.D.; Lee, M.K.; Morrow, J.E.; Welcsh, P.L.; LeoÂn, P.E.; King, M.C. Nonsyndromic Deafness DFNA1 associated with mutation of a human homolog of the *Drosophila* gene diaphanous. *Science* **1997**, *278*, 1315–1318.
113. Medlin, L.; Elwood, H.J.; Stickel, S.; Sogin, M.L. The characterization of enzymatically amplified eukaryotic 16S-like rRNA-coding regions. *Gene* **1988**, *71*, 491–499.
114. An, S.M.; Choi, D.H.; Lee, J.H.; Lee, H.; Noh, J.H. Identification of benthic diatoms isolated from the eastern tidal flats of the Yellow Sea: comparison between morphological and molecular approaches. *PLoS ONE* **2017**, *12*, e0179422.
115. Stamatakis, A. RAxML version 8: a tool for phylogenetic analysis and post-analysis of large phylogenies. *Bioinformatics* **2014**, *30*, 1312–1313.
116. Ronquist, F.; Huelsenbeck, J.P. MrBayes 3: Bayesian phylogenetic inference under mixed models. *Bioinformatics* **2003**, *19*, 1572–1574.
117. An, S.M.; Noh, J.H.; Kim, J.H.; Kang, N.S. Ultrastructural and Molecular Characterization of *Surirella atomus* Hustedt 1955 (Bacillariophyta, Surirellalceae), A Newly Recorded Species in Korea. *Ocean Polar Res.* **2021**, *43*, 245–253.
118. Kang, N.S.; Cho, K.; An, S.M.; Kim, E.S.; Ki, H.; Lee, C.H.; Choi G.; Hong, J.W. Taxonomic and Biochemical Characterization of Microalga *Graesiella emersonii* GEGS21 for Its Potential to Become Feedstock for Biofuels and Bioproducts. *Energies* **2022**, *15*, 8725.

119. Baek, K.; Yu, J.; Jeong, J.; Sim, S.J.; Bae, S.; Jin, E. Photoautotrophic production of macular pigment in a *Chlamydomonas reinhardtii* strain generated by using DNA-free CRISPR-Cas9 RNP-mediated mutagenesis. *Biotechnol. Bioeng.* **2018**, *115*, 719–728.
120. Garces, R.; Mancha, M. One-step lipid extraction and fatty acid methyl esters preparation from fresh plant tissues. *Anal. Biochem.* **1993**, *211*, 139–143.